Shear Flows at the Tokamak Edge and Their Role in Core Rotation and the *L-H* Transition

A. Y. Aydemir

Institute for Fusion Studies, the University of Texas at Austin, Austin, Texas 78712, USA

(Received 29 December 2006; published 1 June 2007)

Pfirsch-Schlüter fluxes in tokamaks are shown to drive strong poloidal and toroidal shear flows that are localized to the edge and scrape-off layer in the presence of temperature gradients and finite bootstrap current in the pedestal. Within a magnetohydrodynamic model, the effect of these flows on core rotation and their role in the magnetic configuration dependence of the power threshold for the low- (L-) to high- (H-)mode transition are discussed. Theoretical predictions based on symmetries of the underlying equations, coupled with computational results, are found to be in general agreement with observations in the Alcator C-Mod tokamak [Phys. Plasmas **12**, 056111 (2005)].

DOI: 10.1103/PhysRevLett.98.225002 PACS numbers: 52.25.−s, 52.65.Kj

Macroscopic flows have a significant effect on transport and stability in tokamaks. In particular, shear flows at the edge play an essential role in the transition from low- (L-) to high- (H-)mode observed in all tokamaks that lead to improved confinement [1–4]. Flows responsible for this desirable enhanced-confinement regime are associated with a negative radial electric field at the plasma edge that becomes more negative during the L-H transition, leading to an increase in the poloidal rotation velocity and its shear. Although the exact mechanism is not well understood, one of the principal drives behind this torque is believed to be the "ion orbit loss" [2]. This effect and others are reviewed in a comprehensive article by Connor and Wilson [5].

Tokamaks in general exhibit other flows not directly associated with the L-H transition. The central (core) region rotates toroidally, especially when the plasma is heated using unbalanced neutral beams that contribute a net toroidal angular momentum to the plasma. Because of its stabilizing influence on macroscopic instabilities like the resistive wall mode, toroidal rotation in tokamaks has received a great deal of theoretical and experimental attention. A puzzling feature of this rotation is its spontaneous occurrence even without an apparent momentum source in purely Ohmic plasmas [6,7], so far without a generally accepted explanation.

Tokamak experiments report flows also in the scrape-off layer (SOL), the narrow layer outside the last closed flux surface that plays the role of an "exhaust" for heat and particles that escape the region of toroidally-nested flux surfaces within the separatrix [8–10]. These flows have been documented in detail in C-Mod [11] in a series of works by LaBombard and coworkers [10,12,13].

All macroscopic flows in different parts of a tokamak do not necessarily have a single physical cause. However, there are ubiquitous "Pfirsch-Schlüter flows" [14], essentially a by-product of toroidal geometry itself, that connect the core plasma to the edge and the SOL. When coupled with other neoclassical effects like the bootstrap current [14], these may have a strong and unifying influence on all of the aforementioned flows in today's and the next generation tokamaks. This point constitutes the main theme of this Letter.

Recently, without explicitly identifying them as Pfirsch-Schlüter flows, Montgomery and co-workers have pointed out that steady-state conditions necessarily include flows, both poloidal and toroidal, when simple nonideal processes are included in a fluid description of toroidal plasmas [15,16]. Since they considered only atypical equilibria with vacuum fields and uniform transport coefficients, the flows they found were of insignificant amplitude. We demonstrate below that the same processes, when examined under more realistic conditions and augmented by neoclassical physics, can generate flows that are orders of magnitude larger, and that they can have a significant impact on toroidal confinement.

In particular, we show that the edge and SOL flows may play an important role in the self spin-up of Ohmic H-mode discharges, as seen in C-Mod and elsewhere [6,7,13]. Since the sign of the momentum input due to these flows depends on the magnetic configuration, they may also provide an explanation for the increased H-mode power threshold under certain conditions [17], which may not necessarily be ∇B drift-dependent, as previously assumed.

Some important characteristics of these flows can be obtained simply from a generalized Ohms' law,

$$-\nabla\phi + \nabla(V_l\zeta) = -\boldsymbol{u}\times\boldsymbol{B} + d_i(\boldsymbol{J}\times\boldsymbol{B} - \nabla p_e) + \eta(\boldsymbol{J} - \boldsymbol{J}_{\rm BS}), \quad (1)$$

where $\boldsymbol{u} \simeq \boldsymbol{v}_i$, $\boldsymbol{J}_{\rm BS}$ is the bootstrap current, and V_l is the loop voltage. A typical magnetohydrodynamic (MHD) normalization with $v_A = B_0/\sqrt{\mu_0 m_i n}$, etc., has been used to put the equation in a nondimensional form so that $d_i = (c/\omega_{pi})/a$, $\omega_{pi}^2 = ne^2/(\epsilon_0 m_i)$, and a is the minor radius. Assuming axisymmetry, we can write $\boldsymbol{B} = \nabla\psi\times\nabla\zeta + F\nabla\zeta$, where ψ is the poloidal flux function $\psi \equiv R^2\boldsymbol{A}\cdot\nabla\zeta$, and $F \equiv R^2\boldsymbol{B}\cdot\nabla\zeta$. Then the covariant components of the Ohm's law in a flux coordinate system (ψ, θ, ζ) can be written as

$$\frac{\mathcal{J}F}{R^2}u^\theta + u^\zeta = \frac{\partial\phi}{\partial\psi} + d_i\left(\frac{\mathcal{J}F}{R^2}J^\theta + J^\zeta - \frac{\partial p_e}{\partial\psi}\right) + \eta J^*_\psi, \tag{2}$$

$$-\frac{\mathcal{J}F}{R^2}u^\psi = \frac{\partial\phi}{\partial\theta} - d_i\left(\frac{\mathcal{J}F}{R^2}J^\psi + \frac{\partial p_e}{\partial\theta}\right) + \eta J^*_\theta, \tag{3}$$

$$-u^\psi = -d_i J^\psi + \eta J^*_\zeta - V_l. \tag{4}$$

where $\mathcal{J} \equiv 1/\nabla\psi\cdot\nabla\theta\times\nabla\zeta$ is the Jacobian, and for convenience, we let $\boldsymbol{J}^* \equiv \boldsymbol{J} - \boldsymbol{J}_{\rm BS}$ in the resistive terms.

First, we show how the basic poloidal flow patterns arise in this model. Assuming velocities are small ($|u| \ll c_s$, where c_s is the sound speed) so that we can use the Grad-Shafranov equation to represent force-balance, with $F = F(\psi)$ only (in general, with $\boldsymbol{u} \neq 0$, $F = F(\psi,\theta)$ [18]), flux-surface average of Eq. (4) leads to $-\langle u^\psi\rangle = \eta(FF' + p'\langle R^2\rangle) - \eta\langle J_{{\rm BS}\zeta}\rangle - V_l$. If we use the simple bootstrap current model [19], $\boldsymbol{J}_{\rm BS} = (\alpha F p'/\langle B^2\rangle)\boldsymbol{B}$, where α is a numerical factor, then we can define the following measure of the radial velocity (note that our $\nabla\psi$ points inward towards the magnetic axis):

$$u_{rad} \equiv -u^\psi + \langle u^\psi\rangle = \eta p'(\psi)(R^2 - \langle R^2\rangle). \tag{5}$$

Here $u_{\rm rad}$ represents a net, toroidally outward, Pfirsch-Schlüter flux in the MHD limit and forms the basis of the flows considered in this work (solid arrows in Fig. 1). Particle conservation implies that these perpendicular flows in the plasma are accompanied by return flows in the SOL (dashed arrows in Fig. 1); the poloidal projection of the complete flow has a dipole pattern [15]. In an up-down symmetric system, the half above the midplane is in the counterclockwise direction for a monotonically decreasing pressure profile, fixed by toroidal geometry, independent of the direction of the fields and currents. It is accompanied by a clockwise flow below the midplane. For a "normal" configuration of the plasma current and toroidal field, with the ion ∇B-drift towards the field null in a lower single-null (LSN) geometry, the toroidal projection of the flow in the SOL (essentially a parallel flow) is positive above the midplane and negative below.

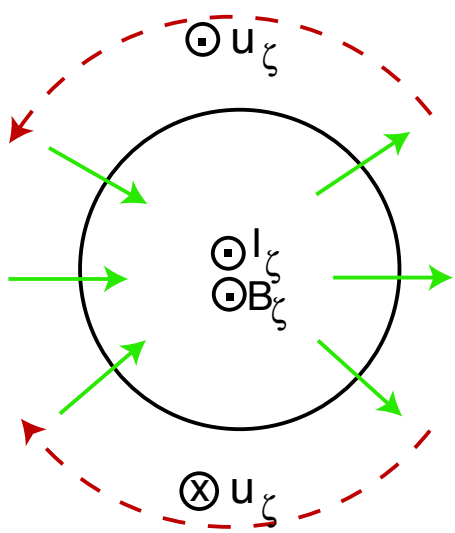

FIG. 1 (color online). Pfirsch-Schlüter flows (solid arrows) and the parallel return flows in the SOL (dashed arrows) that accompany them. For the normal plasma current and toroidal field configuration shown here, the toroidal projection of the parallel flows has to be positive above the midplane and negative below.

Next, we formally examine symmetries of the system, i.e., transformations that leave Eqs. (2)–(4) invariant, in order to understand the changes that occur when current or field directions are reversed. For this purpose, we define a "parity" factor σ_f associated with each variable f such that $\sigma_f^2 = 1$ and $\sigma_f = -1$ implies reversal of the variable: $f \to -f$. For instance, in order to leave Eq. (4) invariant, any set of parity transforms has to satisfy the relations $\sigma_{u^\psi} = \sigma_{d_i}\sigma_{\mathcal{J}}\sigma_F\sigma_\theta = \sigma_{J^*_\zeta}$. All relationships of this form derived from Eqs. (2)–(4) can be combined and reduced to the following:

$$\sigma_{u^\psi} = \sigma_\psi, \qquad \sigma_{u^\theta} = \sigma_\theta, \qquad \sigma_{u^\zeta} = \sigma_\zeta\sigma_F\sigma_\psi, \qquad \sigma_\phi = \sigma_{d_i} = \sigma_\zeta\sigma_F. \tag{6}$$

Note that $u^\psi = \boldsymbol{u}\cdot\nabla\psi$, $u^\theta = \boldsymbol{u}\cdot\nabla\theta$ changes sign only with the basis vectors $\nabla\psi$, $\nabla\theta$, which does not imply an actual change in the flow velocity $\boldsymbol{u}$ itself. However, the toroidal component depends on the direction of the plasma current I_p and toroidal field B_T also: projection of the SOL flow onto the poloidal plane has to be in the direction of the dashed arrows in Fig. 1, which also determines the sense of the toroidal projection.

Keeping Eq. (6) and Fig. 1 in mind and summarizing, we see that no set of transformations of the fields and currents alone will change the direction of the poloidal flow. For fixed $\nabla\zeta$, the toroidal component of the velocity reverses when ψ (all toroidal currents) or F (toroidal field) is reversed, but not when both change sign simultaneously.

Another important transformation involves switching from a LSN to USN (upper-single null) configuration. This change is accomplished (in an abstract sense) by a rotation of the torus by 180° that flips it upside down, followed by a reversal of all toroidal currents and toroidal field. Rotation corresponds to a parity transform ($\boldsymbol{x} \to -\boldsymbol{x}$) in the poloidal plane that results in $\theta \to \pi + \theta$, $\zeta \to \pi - \zeta$ and reversal of the fields. Following the rotation with $\psi \to -\psi$, $F \to -F$ leads to $\boldsymbol{B} \to \boldsymbol{B}$, $\boldsymbol{J} \to \boldsymbol{J}$, $\boldsymbol{u} \to \boldsymbol{u}$ but with the magnetic geometry flipped from LSN to USN. Thus, the flow is not affected directly by this change; however, its interaction with the fields is altered in an important way, as we will see below. Note that since $\psi = \psi_p + \psi_{\rm ext}$, $\psi \to -\psi$ implies reversal of all toroidal currents, including those responsible for the field null.

Next, we turn to a discussion of numerical calculations of these flows, their interpretation in terms of the symmetries shown above, and their comparison with experimental observations.

Figure 2 shows the quasisteady edge and SOL flows in various magnetic geometries, self-consistently generated within an MHD model using the Ohm's law in Eq. (1) with $d_i = 0$ and $J_{BS}/J_0 \simeq 0.2 - 0.3$, where J_0 is the current density on axis. The dipole structure of the flows that is suggested by Eq. (5) is evident in the DN configuration [Fig. 2(a)], both in the poloidal and toroidal components of the velocities. In DN, the flows are antisymmetric with respect to the midplane and carry no net toroidal angular momentum. In the USN and LSN configurations, the basic flow patterns are essentially repeated, consistent with Eq. (6), but with modifications introduced externally by the asymmetric field geometry. In Fig. 2(b) (USN), the poloidal flows in the lower half of the poloidal plane have expanded past the midplane at the expense of those in the upper half, which have now been altered. Interaction of the flow with the line-tied open field lines around the X-point damps the toroidal flow there, leaving behind a net negative (countercurrent) momentum input in the lower half of the poloidal plane. In Fig. 2(c) (LSN), the effect is reversed, now providing a net positive (cocurrent) toroidal momentum contribution. Both the sense and location of momentum input (the edge) are consistent with the observations in C-Mod [10,12].

Thus, asymmetric damping of one half of the toroidal dipole seen in Fig. 2(a) through its interaction with the single-null point in LSN or USN provides an explanation for the "self spin-up" of Ohmic discharges without an apparent external momentum source [6,7,13]. Since the Pfirsch-Schlüter flux responsible for these antisymmetric flows are part of tokamak plasmas in all collisionality regimes, this is a robust and universal mechanism for momentum input to toroidal plasmas. However, the source is localized to the edge; how momentum is transported from the edge inward is not clear and is not addressed in this Letter. An experimental check for the validity of this mechanism as a toroidal momentum source would be the following: since the source is vertically asymmetric, located opposite from the active null point, in steady-state the toroidal velocity profile should also be sheared in the same direction.

Our calculations also support the conjecture by LaBombard *et al.* [10] that the edge-generated toroidal flows can explain the increased power requirements for the L-H transition observed under certain conditions. If we assume (a) toroidal rotation is involved in the transition, and (b) there is an independent cocurrent rotation drive in the core, for example, due to rf heating [20], then the toroidal momentum input from the Pfirsch-Schlüter flows adds to that by the heating source in the normal LSN configuration [Fig. 2(c)] and opposes it in the USN [Fig. 2(b)], or when both I_p and B_T are reversed in LSN.

At this point, based on the symmetry arguments and the calculations presented here, we can make a couple of experimentally testable predictions. Starting in the normal configuration and reversing only the toroidal field in LSN should also reverse the toroidal momentum input, thus making it more difficult to enter H-mode. Also, since reversing both I_p and B_T while maintaining LSN does not affect the flows, if heating, for example due to neutral beams, continues to input momentum in the original (now countercurrent) direction, the power threshold should not be affected, although the ∇B drift now would point away from the X-point.

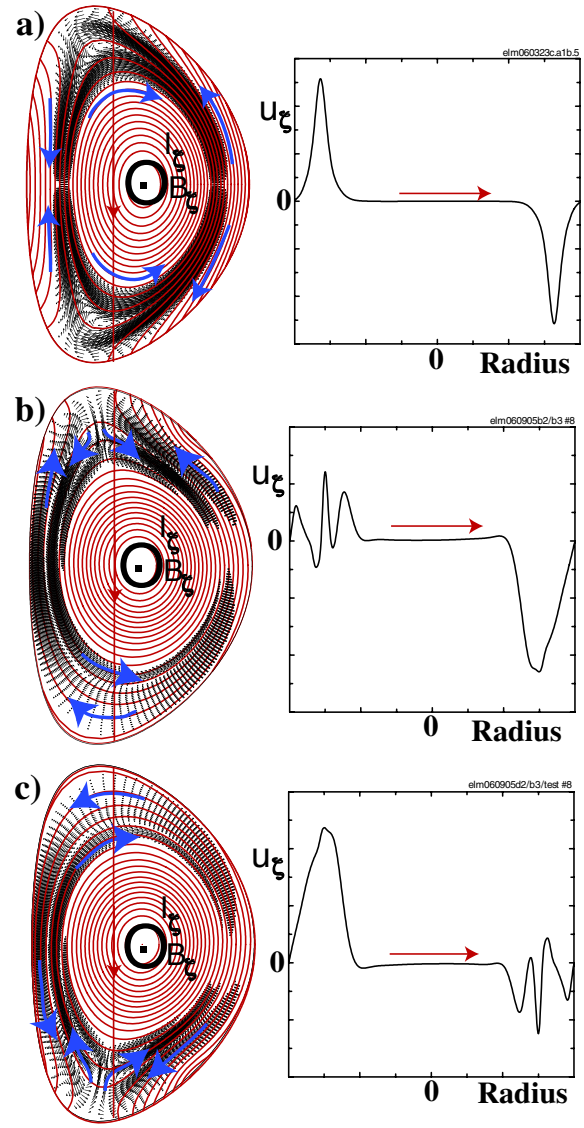

FIG. 2 (color online). Edge and SOL flows in various field geometries. (a) Double-null (DN), (b) Upper single-null (USN), (c) Lower single-null (LSN). Toroidal velocities are plotted along the vertical lines shown on the left, starting from the top of the torus.

The poloidal flow patterns in Fig. 2 are qualitatively consistent with the experimental observations (e.g., Fig. 16 in Ref. [10]), in particular, with those identified as "transport-driven" flows. In all configurations, but most clearly in the DN, there is a stagnation point approximately at the outboard midplane. There are also strong flows from the outboard to the inboard SOL both in LSN and USN,

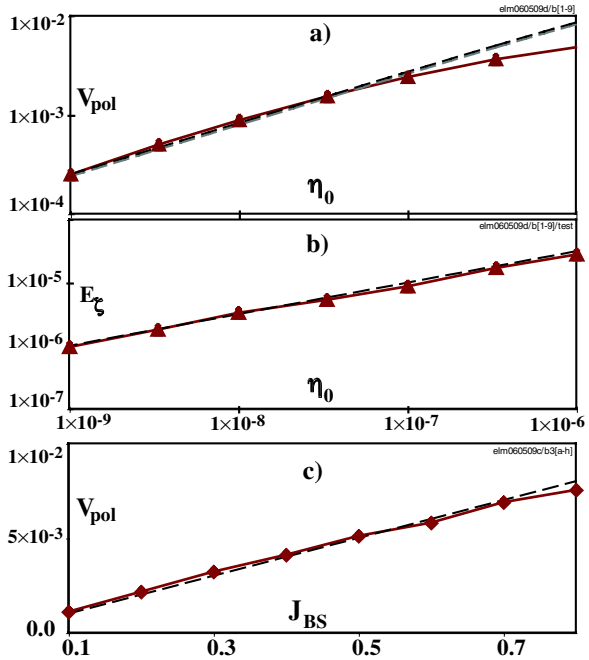

FIG. 3 (color online). Scaling of the poloidal flows with resistivity and the bootstrap current. Average toroidal $\beta = 5 \times 10^{-5}$ for all cases. (a) Maximum of the poloidal velocity, $V_{\rm pol} \equiv |\boldsymbol{u}_{\rm pol}|_{\rm max}$, as a function of η_0, resistivity on axis. For this scan $\eta_{\rm edge}/\eta_0 = 10^5$. Here and in (b) below, the dashed line illustrates an exact $\eta^{1/2}$ scaling. (b) Scaling of the electric field $E_\zeta \equiv \eta(J_\zeta - J_{{\rm BS}-\zeta})$ at the outboard midplane with resistivity. (c) Scaling of $V_{\rm pol}$ with the bootstrap parameter $J_{\rm BS}$ at fixed $\eta_0 = 10^{-6}$. Here the dashed line has unit slope.

directed towards the inner strike point of the divertor, independent of the direction of I_p and B_T [10].

Localization of the flows around the separatrix is due to the parallel electric field associated with the bootstrap current and resistivity gradient at the edge; without these, the dipole flow patterns persist but are more diffuse, similar to those reported in Ref. [16]. Figure 3 summarizes scaling of these flows with resistivity and bootstrap current fraction at fixed β. In Fig. 3(a), maximum poloidal velocity, $V_{\rm pol} \equiv |\boldsymbol{u}_{\rm pol}|_{\rm max}$, is plotted as a function of resistivity. In the absence of bootstrap current contribution, the expected scaling is linear; however, with finite $J_{\rm BS}$, it is clearly $\eta^{1/2}$ for small η_0. This scaling is consistent with that of the toroidal electric field $E_\zeta \equiv \eta(J_\zeta - J_{{\rm BS}-\zeta})$ shown in Fig. 3(b). It follows from the following simple scaling argument: $(J_\zeta - J_{{\rm BS}-\zeta}) \sim B/\delta$, where the width $\delta \sim \eta^{1/2}$. It is also consistent with the expectation that the total current density $J \to J_{\rm BS}$ only in the limit $\eta \to \infty$. (Recall that $J_{\rm BS}$ is essentially a free parameter here.) Poloidal flows scale linearly with the bootstrap current amplitude, as seen in Fig. 2(c), where we plot the maximum poloidal velocity $V_{\rm pol}$ again, but at fixed resistivity as we increase $J_{\rm BS}$. There are indications that the flow amplitude scales linearly with β, which would be consistent with Eq. (5); however, a clear confirmation of this trend is left for a future work.

We conclude by pointing out once more that the self-consistent flows considered here have their origin in the toroidal geometry itself; thus, the direction of their poloidal projection is independent of the field or current directions, although the toroidal velocity does depend on the magnetic configuration.

This work was supported by the U.S. Department of Energy, Office of Fusion Energy Sciences. Computational resources were provided by the National Energy Research Scientific Computing Center, also supported by the U.S. Department of Energy.

[1] K. C. Shaing, Phys. Fluids **31**, 2249 (1988).
[2] K. C. Shaing and E. C. Crume, Phys. Rev. Lett. **63**, 2369 (1989).
[3] R. J. Groebner, K. H. Burrell, and R. P. Seraydarian, Phys. Rev. Lett. **64**, 3015 (1990).
[4] K. H. Burrell, Plasma Phys. Controlled Fusion **36**, A291 (1994).
[5] J. W. Connor and H. R. Wilson, Plasma Phys. Controlled Fusion **42**, R1 (2000).
[6] I. H. Hutchinson, J. Rice, R. S. Granetz, and J. A. Snipes, Phys. Rev. Lett. **84**, 3330 (2000).
[7] A. Bortolon, B. P. Duval, A. Pochelon, and A. Scarabosio, Phys. Rev. Lett. **97**, 235003 (2006).
[8] N. Asakura, S. Sakurai, K. Itami, O. Naito, H. Tagenaga, S. Higashijima, Y. Koide, Y. Sakamoto, H. Kubo, and G. D. Porter, J. Nucl. Mater. **313**, 820 (2003).
[9] R. A. Pitts, P. Andrew, X. Bonnin, A. V. Chankin, Y. Corre, G. Corrigan, D. Coster, I. Duran, T. Eich, and S. K. Erents *et al.*, J. Nucl. Mater. **337**, 146 (2005).
[10] B. LaBombard, J. E. Rice, A. E. Hubbard, J. W. Hughes, M. Greenwald, J. H. Irby, Y. Lin, B. Lipshultz, E. S. Marmar, and C. S. Pitcher *et al.*, Nucl. Fusion **44**, 1047 (2004).
[11] I. H. Hutchinson and the Alcator C-Mod Group, Phys. Plasmas **1**, 1511 (1994).
[12] B. LaBombard, J. E. Rice, A. E. Hubbard, J. W. Hughes, M. Greenwald, R. S. Granetz, J. H. Irby, Y. Lin, B. Lipshultz, and E. S. Marmar *et al.*, Phys. Plasmas **12**, 056111 (2005).
[13] J. E. Rice, A. E. Hubbard, J. W. Hughes, M. J. Greenwald, B. LaBombard, J. H. Irby, Y. Lin, E. S. Marmar, D. Mossessian, and S. M. Wolfe *et al.*, Nucl. Fusion **45**, 251 (2005).
[14] F. L. Hinton and R. D. Hazeltine, Rev. Mod. Phys. **48**, 239 (1976).
[15] L. P. Kamp and D. C. Montgomery, Phys. Plasmas **10**, 157 (2003).
[16] L. P. Kamp and D. C. Montgomery, J. Plasma Phys. **70**, 113 (2004).
[17] F. Ryter and the H Mode Database Working Group, Nucl. Fusion **36**, 1217 (1996).
[18] E. Hameiri, Phys. Fluids **26**, 230 (1983).
[19] R. L. Miller, Y. R. Lin-Liu, A. D. Turnbull, V. S. Chan, L. D. Pearlstein, O. Sauter, and L. Villard, Phys. Plasmas **4**, 1062 (1997).
[20] L.-J. Zheng and J. W. VanDam (private communication).